Experimental and numerical study of a modified ASTM C633 adhesion test for strongly-bonded coatings

Raphaelle Bernardie, Reda Berkouch, Stéphane Valette, Joseph Absi, Pierre Lefort

Experimental and numerical study of a modified ASTM C633 adhesion test for strongly-bonded coatings †

Raphaëlle Bernardie, Reda Berkouch, Stéphane Valette, Joseph Absi* and Pierre Lefort

University of Limoges, SPCTS, UMR CNRS 7315, 12, Rue Atlantis F-87068 Limoges Cedex, France

When coatings are strongly bonded to their substrates it is often difficult to measure the adhesion values. The proposed method, which is suggested naming "silver print test", consists in covering the central part of the samples with a thin layer of silver paint, before coating. The process used for testing this new method was the Air plasma spraying (APS), and the materials used were alumina coatings on C35 steel substrates, previously pre-oxidized in CO_2. The silver painted area was composed of small grains that did not oxidize but that significantly sintered during the APS process. The silver layer reduced the surface where the coating was linked to the substrate, which allowed its debonding, using the classical adhesion test ASTM C633-13, while the direct use of this test (without silver painting) led to ruptures inside the glue used in this test. The numerical modelling, based on the finite element method with the ABAQUS software, provided results in good agreement with the experimental measurements. This concordance validated the used method and allowed accessing to the values of adherence when the experimental test ASTM C633-13 failed, because of ruptures in the glue. After standardization, the "silver print test" might be used for other kinds of deposition methods, such as PVD, CVD, PECVD.

Keywords: Adhesion measurements; Strongly-bonded coatings; Silver print test; Numerical simulation; Finite element method

1. Introduction

Surface coating technology presents interesting opportunities in the industry by, for example, increasing the resistance to corrosion, improving the special magnetic or electrical properties. It should be noted that the performance and reliability of the coatings depend on the mechanical characteristics of the coating/substrate interface. The adhesion mechanisms of the coating can be classified as: (a) Interfacial adhesion in which the adhesive forces are centered around a well-defined thin interface; (b) interdiffusion adhesion in which the coating and the substrate diffuse into one another with a thicker interfacial region; (c) intermediate layer adhesion in which the coating and the substrate are separated by one or more layers of materials of different chemical compositions; (d) mechanical interlocking adhesion in which the coating/substrate interface is relatively rough [1]. A good understanding of the adhesion and damage mechanisms of the coating/substrate systems is necessary to achieve the full potential of the coatings. Thus, it is necessary to develop reliable techniques for evaluating the adhesion of the coating.

In the case of thick coatings strongly bonded to substrates, (e.g. adhesions higher than ca. 60 MPa), the adhesion values cannot be easily measured, despite the numerous methods of measurements [2, 3]. In fact, in many cases, such as the coating of ceramics on metallic substrates by thermal plasma spraying, the adherence is poor, or medium [4]. So, the adhesion value of coatings can be classically determined via a conventional tensile test. The measurements are carried out with a tensile testing machine, following typically the ASTM test C633, developed for a long time [5-7]. In this test, the samples must be plane with two parallel faces, one being covered by the coating, and the other remaining bare. For the tensile tests, both faces are glued on two cylindrical dollies, put in the tensile machine, with pulling rates generally low, below 1 mm/min. The rupture strength σ_r, is defined by the ratio (1) of the force reached at breaking, F_b, to the area of the coating/substrate interface, $A_{C/S}$:

$$\sigma_r = F_b / A_{C/S} . \quad (1)$$

The adhesive used has always a high tensile strength (> 50 MPa), and both the traction dollies and the not-covered surface of the samples are previously sandblasted, in order to improve the adherence of the glued pieces [6].

*Corresponding author. Tel.: +33 587502557, Fax.: +33 587502304
E-mail address: joseph.absi@unilim.fr

Now, the progresses in the treatment of the interfacial zones provide coatings more and more strongly bonded to the substrates, so that, when using the classical test ASTM C633, the breakings occur inside the glue instead of inside the sample. In these conditions, a new and very simple method modifying the tensile test ASTM C633-13 has been implemented. It consisted just in lowering the area of the coating/substrate interface (AC/S) by painting partially the substrates with a thin layer of silver paint before coating. A numerical modelling of this method has been carried out based on finite element method.

2. State of the art

Several mechanical testing methods [2-4, 8-14] have been developed to evaluate the adhesion of coatings, in particular of plasma coatings. Among the most widespread tests, the pin test [8], the interfacial indentation test [9, 10], the shear adhesion test [11], the peel adhesion test [12], the bending tests (three or four points [10]) and the double cantilever beam (DCB) test [2]. The tensile adhesion test standardized ASTM C633 [5] is the most commonly used method, because of its simplicity and of its reliability. However, if the coatings reach adhesion values greater than the strength of the adhesive used (higher than about 50 - 60 MPa), the failures occur inside the adhesive layer and thus the value of the coating adhesion cannot be determined. In order to bypass this difficulty, several experimental studies [13, 14] have proposed modifications of the tensile adhesion test.

Qian et al. [13] introduced, during the process of thermal spraying, a very thin circular carbon layer, simulating a crack inside the coatings. The carbon layer was penny-shaped, 5 mm in diameter, and located at different depths of the Thermal barrier coatings (TBCs): This promotes the crack propagation at lower tensile load.

On the same bases, Kishi et al. [8] modified the pin test by covering the rim of the samples by a thin circular carbon layer, put with a pencil, using a lathe. The so-modified pin test does not require an adhesive and it could be considered relevant for evaluating the adhesion of thermal sprayed coatings, but the samples configuration is rather complicated, and the implementation is delicate.

Watanabe et al. [14] used the same ring-shape carbon layer than Kishi et al. [8], but the deposition process is the High velocity Oxy-fuel (HVOF) that induces severe deformations of the sample edges. Hence this technique appears as well suited only insofar as the deposit temperatures remain rather low and because carbon covers the eroded edges of the samples. At the opposite, with the thermal plasma coating processes (Air plasma spraying, APS) where temperatures are rather high during plasma spraying, the carbon layer is oxidized in CO_2, at least partially.

Seen these difficulties, it was necessary to implement a new modification of the existing tests, especially suited for the plasma spraying process.

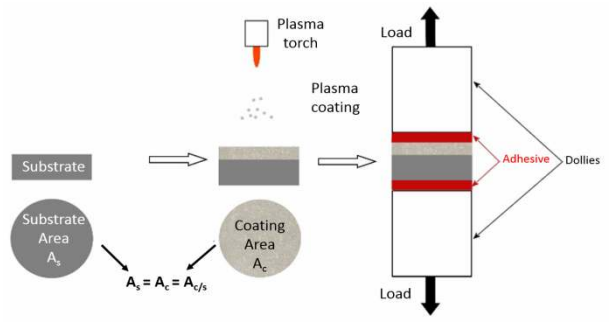

Fig. 1. The classical test ASTM C633; $A_{C/S}$ is the area of the interface coating/substrate.

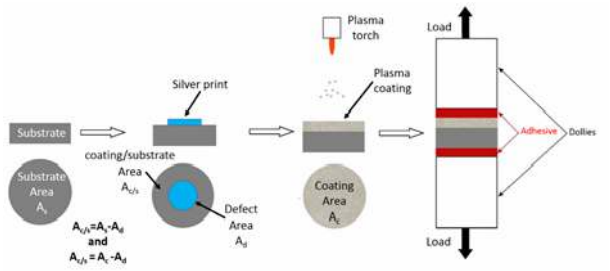

Fig. 2. The modified test ASTM test C633 with the "silver print test".

3. Experimental

3.1 Principle

Usually, in the ASTM C633-13 test (see Fig. 1), the area of the interface {coating/substrate} (area $A_{C/S}$) is the same than that of the interface {coating/glue} (area $A_{C/G}$), and the same than that of the interface {substrate/glue} (area A_S).

As seen before, for the very strongly-bonded coatings, the rupture strength, σ_r, of the interface {coating/substrate} becomes higher than the cohesion C_g of the glue, or higher than the adhesion of the sample onto the dollies, so that the ruptures occur inside the glue or at the interfaces sample/dollies. In order to measure the coating adhesion, the rupture load (F_b) required for debonding the coatings must be always lower than that necessary for the rupture inside the glue. This is only possible if, for the same rupture load F_b, the area substrate/coating ($A_{S/C}$) is smaller than the areas of the coating A_C and of the substrate (A_S). The simplest solution for reducing the area substrate/coating ($A_{S/C}$) should be to cover only partially the substrate by the ceramic coating, but this was not experimentally easy with the usual coatings methods (CVD, PVD, PECVD...). Moreover when gluing:

(1) On the partially coated side, the glue necessarily covers both the coated area $A_{S/G}$ and the uncoated area, which make difficult the interpretation of the results;

(2) The deposit becomes thinner at the boundary coated/uncoated areas (it does not stop abruptly), and it is impossible to estimate accurately the actual area coated;

(3) The uncoated area must be as centrosymmetric as possi-

ble, at the sample surface, in order to avoid any dissymmetry of the stresses during the traction test; this is very difficult to obtain during the coating.

Considering these restraints, and the necessity of an experimental implementation as simple as possible, a mask composed of silver paint was placed onto the surface of the sample, before coating, in order to prevent the adhesion of the coating on the masked zone. The three main advantages expected of the silver paint are the following:

(i) It is easy to put onto the samples with a simple brush;

(ii) It is very common, as far as it is classically used during the preparation of samples for electronic microscopy;

(iii) It has a melting point of 962 °C, the highest thermal conductivity of all the metals (about 430 W m^{-1} K^{-1}), and a very good resistance against oxidation in air [15]: It is supposed able to resist to the impact of the sprayed molten particles, even in the case of ceramics with high melting points. Fig. 2 presents schematically the sample configuration in the modified adhesion test ASTM C633-13. The defect region corresponds to the silver print (area noted A_d).

3.2 Choice of the samples

Samples were low carbon steel C35 provided by Outil-Metal S.A. (Limoges, France), pre-oxidized in CO_2 and covered with alumina by thermal plasma coating process [9]. This multilayered material is known for the high quality of the junction ceramic/metal due to the "crystallographic bonding" that guarantee smooth physical and chemical transitions between the different phases without any gap of properties, with the phases sequence: Steel/α-iron/wüstite/magnetite/γ-Al_2O_3/α-Al_2O_3. An example of industrial applications of such multilayer system can be encountered in waste-to-energy plant [16].

3.3 Painting method

The silver mask was a paint provided by Provac (France), reference PRHC 140 20. It was manually put on the sample with a brush, using a stencil, with a circular hole centred in the middle of the pre-oxidized discs. The circular shape of the painted area was chosen for limiting the shear forces that appear during the tensile tests, for non-centrosymmetric shapes. The painting step took place after the pre-oxidation in CO_2, and just before the APS. In the illustration of Fig. 3(a), the masked zone had a diameter of 12 mm, but this diameter could be larger or smaller. After drying during 12 h at 20 °C, the mask was a continuous layer (about 8 to 10 µm thick) of submicron silver grains gathered in aggregates, illustrated in the micrograph of Fig. 3(b). During the first step of the APS process, samples were pre-heated in air by the plasma jet at ca. 600 K during 90 s, for removing adsorbates and condensates from the surface. The pre-heating temperature and duration were strictly limited to these values because, for more drastic treatments, the wüstite layer completely converts into magnetite (Fe_3O_4) and very brittle hematite (Fe_2O_3), giving poorly adhering alumina coatings [17].

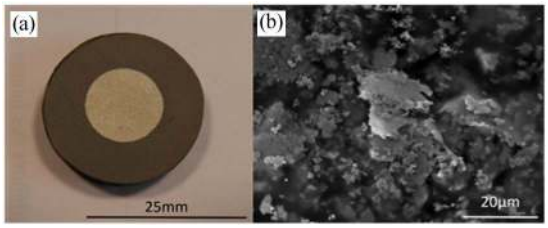

Fig. 3. Sample partially covered by the silver mask before APS: (a) Surface covered by a disc of silver paint (clear zone); (b) detail of the surface of the painted zone.

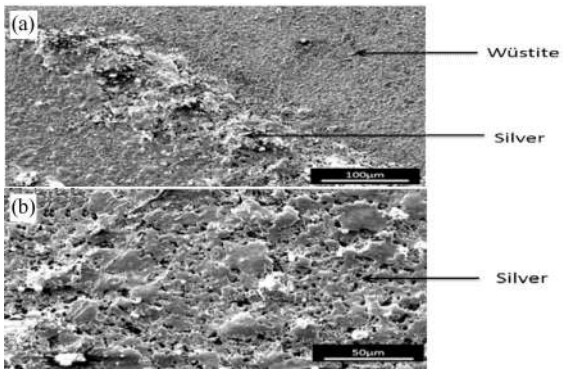

Fig. 4. SEM observations of the surface sample after plasma preheating: (a) The limit of the silver mask; (b) the silver surface.

The wüstite/silver limit (Fig. 4(a)) remained well defined and the layer was regular with a significant porosity (Fig. 4(b)). During the last step (plasma spraying), the samples were impacted by molten alumina particles at a temperature higher than 2072 °C (melting point of alumina). After this coating process, we can observe, in a cross section of a sample, the following results: (i) The silver mask remained always unchanged, as it can be seen in Fig. 5(a), (ii) a sharp border between the three compounds: alumina, wüstite, silver as we can observe in Fig. 5(b). In this zone we can also remark that no spreading of silver takes place at the wüstite/alumina interface. Moreover, a test was made in order to check that the alumina coating does not adhere to the silver paint. For this, the surface of a sample was entirely painted, and then alumina coated. After cooling, the alumina layer was hand pulled off very easily, and on this basis it was admitted that the adhesion of the coating to the substrate was nil on the painted zones of the samples.

4. Results and discussion

4.1 Mechanical tests

The ASTM test method C633-13 defines the following conditions only applicable in the case of thermal spray coatings:

- A pulling rate between 0.013 mm/s and 0.021 mm/s,
- A facing diameter between 23 and 25 mm,

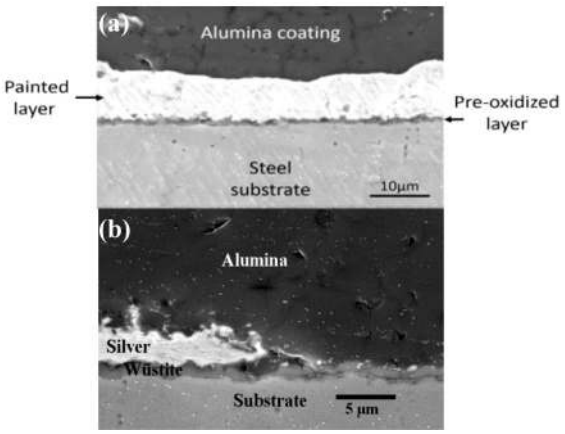

Fig. 5. SEM observations in cross section of a steel disc with a silver painted zone between the substrate and the alumina coating: (a) Zone entirely covered by the silver paint; (b) border zone of the three compounds.

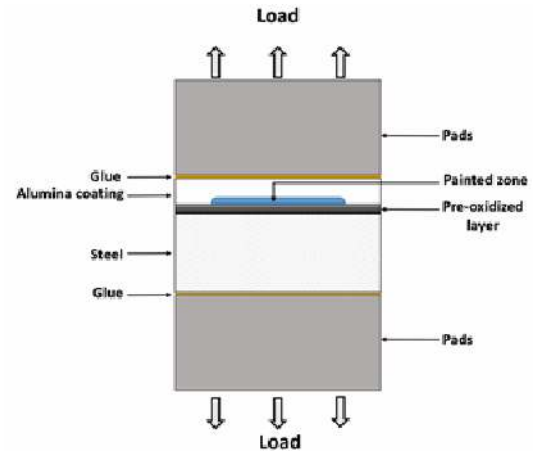

Fig. 6. Schematic cross-section of a sample to be tested (not real scale).

- A coating thickness greater than 380 µm. However, the minimum thickness value can be modulated with the nature of the bonding agent. In order to improve the adhesion of the glue, the steel substrates were grit blasted on the side where they were not coated. Then the samples were glued on both their faces onto two cylindrical dollies (diameter = 25 mm, length = 35 mm), which were also grit blasted for best sticking. According to the supplier's recommendations (HTK Hamburg, Germany), the thermosetting glue (HTK Ultra Bond 100) was polymerized for 120 min at 150 °C. 10 samples of pre-oxidized steel coated with alumina were tested, with silver painted areas 16 mm in diameter, and 10 others without silver mask. A tensile testing machine (Adamel-Lomargy DY-26, France) was used for the mechanical test, following the recommendation sited upper : Pulling rate = 0.013 mm/s; samples diameter = 25 mm and coating thickness = ca. 400 µm.

Fig. 6 gives a schematic representation (in cross-section) of a sample glued on the dollies just before testing. As expected, the breaking always occurred inside the samples, at the interface substrate / coating, instead of inside the glue for the non-painted samples. This allowed determining the adhesion value of 82 ± 7 MPa, the uncertainty corresponding to a confidence interval of 95 % [18]. Without silver masks, the ruptures always occurred inside the glue, which shows the utility of the ASTM C633-13 modified test, which has been suggested to be named "silver print test".

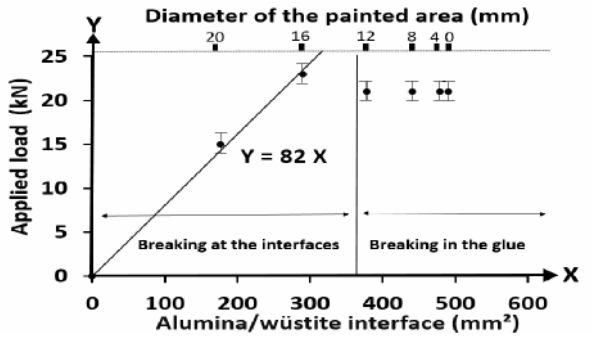

Fig. 7. Applied load to rupture for alumina-coated steel samples, according to the non-painted area (alumina/wüstite interface) or to the diameter of the painted area, from Ref. [18].

Several other tests were carried out with painted areas of different diameters, each time with 10 samples:

(1) When the painted zone was larger (20 mm), the ruptures occurred again inside the samples but for a lower value of load;

(2) At the opposite, for smallest diameters of the painted zone (12, 8 and 4 mm), the ruptures occurred in the glue.

These results are summarized in Fig. 7 that represents the applied load at the rupture vs. the area of the alumina/substrate interface, i.e. the useful area of the coating (or vs. the diameter of the painted area). Hence, for the samples of the present study the best painted area diameter is 16 mm, but, for other kinds of strongly-bonded coatings, the area of the painted zone must be adapted both to the values of the glue cohesion (here estimated around 100 MPa) and to the adhesion/cohesion of the tested pieces.

4.2 Numerical approach

In order to confirm the experimental value of adherence (σ_r = 82 ± 7 MPa) obtained with the "silver print test", and, consequently to validate the modified ASTM C633-13 adhesion test, the modelling of the assembly was implemented by the finite element method. It was particularly important to demonstrate the capability of the model to take into account the specificities of each layer composing the assembly, especially in order to extrapolate results to zones that could not be reached by the experimental measurements (due to the ruptures inside the glue).

Calculations were carried out with the commercial ABAQUS software with its standard version and Lagrangian finite element formulation. The geometrical model was composed of three superposed cylindrical layers representing re-

spectively the alumina, the wüstite and finally the steel substrate.

4.2.1 Conditions of the finite element simulation of the modified traction test

The general conditions were:

(1) Dimensions: 25 mm in diameter for the three materials, and 300 µm, 2 µm and 5 mm depth respectively for the alumina, wüstite and steel layers;

(2) Modeling of the silver mask: A debonding zone, disc shaped, was created between the alumina and the wüstite layers. The radius R of this zone varied in respect to the experimental values used previously ($0 \leq R \leq 10$ mm); the mechanical characteristics of the three materials used in the numerical process are summarized in Table 1.

(3) The steel/wüstite interface and the rest of the alumina/wüstite interface were in cohesive state. The "TIE" function present in ABAQUS software, was used to create this adhesion state.

(4) Boundary conditions: the lower base of the steel layer was blocked in the vertical direction while the upper circular surface of the alumina was submitted to a vertical displacement as experimentally imposed ($\Delta l = 0.0042$ mm) during the total time of simulation (1 unit of time);

(5) For the meshing operation: the 4-node stress element bilinear axisymmetric with a free quadrilateral shape (CAX4R with 4 nodes) were chosen to optimize the calculations. Refined mesh strategy around the crack tip was adopted. Basic single bias was used in the sizing mesh control on the length and width of the parts. The mesh density was controlled by the thickness of the wüstite layer (2 µm); four subdivisions at least were present in the thickness of this layer. For both the sides of the boundary alumina / steel, the same density of meshing was used, but the mesh density was decreased close to the upper and lower bases, and a refinement was systematically implemented close to the interfacial debonding zone. A convergence test in terms of time and mesh element number is presented in Table 2.

(6) Given the cylindrical geometry of the assembly, representative axisymmetrical configurations of the three layers were chosen in order to reduce the time of calculation. Fig. 8 illustrates the general conditions of the modelling;

At the end of the numerical calculation step, cartographies of the mechanical stresses of the assembly were obtained. Fig. 9 provides an example of a meshed microstructure under mechanical loading and the corresponding stresses mapping. The stresses isovalues are lobes with a dissymmetry due to the different mechanical characteristics of the regarded layers, and the highest level of stresses value is reached at the crack tip.

4.2.2 Numerical results and discussion

Six numerical models with the radius of the silver mask ranging in the interval [0 ; 10 mm] were studied. For each one, the stresses distribution in the whole assembly was analyzed.

Table 1. Mechanical characteristics of alumina, wüstite and steel used in ABAQUS.

Material	Young's modulus (GPa)	Poisson's ratio
Alumina	400	0.27
Wüstite	130	0.33
Steel	210	0.30

Table 2. Convergence test in terms of time and mesh element number under ABAQUS software (7954 is the chosen mesh element number).

Number of elements	Time (CPU)	σ_{22}(MPa) (Crack tip)
1148	12	16,4
4000	14	75
7954	17	78
18450	25	78
61254	63	78

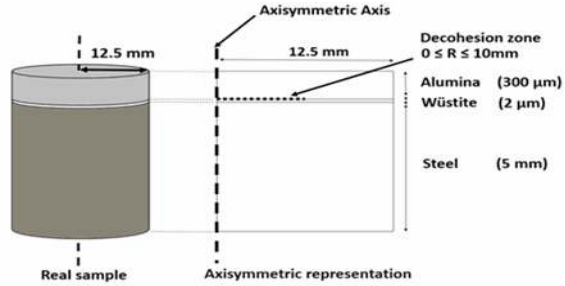

Fig. 8. General conditions of the modeling, with the axisymmetrical representation of the cylindrical geometry.

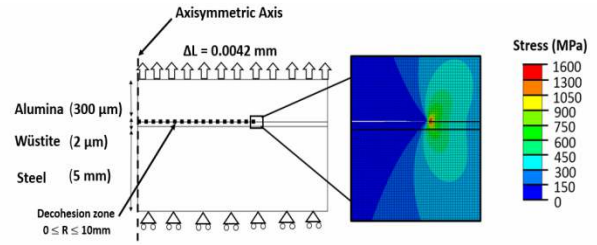

Fig. 9. Stresses mapping around the crack tip under mechanical load.

Particularly, by focusing on the interfacial zone, the changes of the stress distribution along the cohesive zone were observed. The results are given in Table 3.

Whatever the silver mask size, the stresses reached always very high values (> 1000 MPa) at the triple point: silver mask / wüstite / alumina, and the stresses isovalues are always dissymmetrical. The stresses decrease very strongly with the distance d to the triple point, and they reach the asymptote of about 78 MPa for distances varying from 0.1 to 0.2 mm when the silver mask diameter increases from 4 to 20 mm. This variation is in relationship to the width of the ring where alumina and wüstite are in contact but the origin of this relationship is not clear. The value of 78 MPa represents the adhesion

Table 3. Stresses mapping and values according to the distance d to the crack tip for different sizes of silver masks.

Stresses mapping (MPa)	Stresses (*S*) according to the distance to the crack tip (*d*)
Diameter of silver area:4 mm 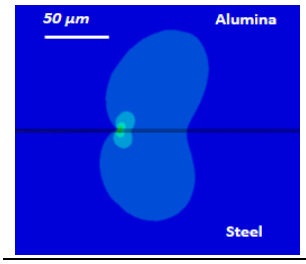	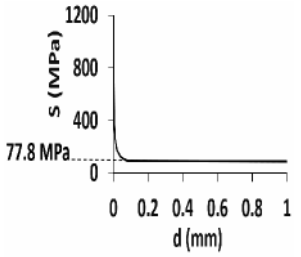
Diameter of silver area: 12 mm 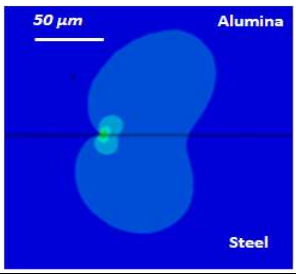	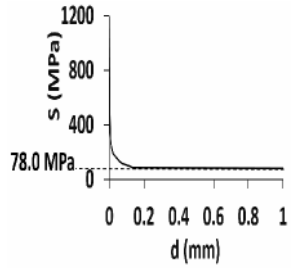
Diameter of silver area: 20 mm 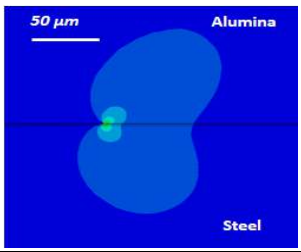	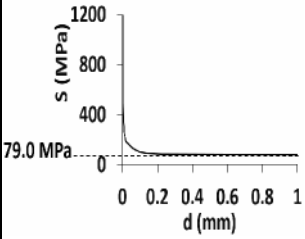

of the alumina coating. It is included in the experimental confidence interval of 82 ± 7 MPa, which constitutes a first validation of the modeling.

Now, regarding the calculated values of the load to rupture, deduced from the stresses to rupture of Table 3, Fig. 10 presents the expected convergence between numerical and experimental values, when the rupture takes place at the interface coating / substrate. When the rupture occurred in the glue (experimentally), the calculation allows determining the value of the load to rupture of the coating, in a zone not accessible experimentally, which reaches the high value of 37.8 kN for the sample without silver mask.

5. Conclusion

On the basis of steel samples, alumina coated by APS, and having a coating adherence of about 80 MPa, the mechanical test ASTM C633-13, modified by the "silver print test" showed its capability for measuring the values of coatings adhesions, when the bonding to the substrates is too strong for using directly the usual test ASTM C633-13. The feasibility of this modified method has been confirmed both experimentally, and by numerical simulation.

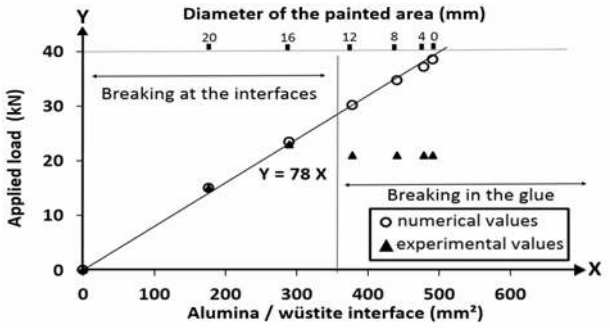

Fig. 10. Numerical / experimental comparison of the loads to rupture for the different sizes of the silver mask.

For the numerical part, the commercial ABAQUS software was used with a model implying the 3 layers present in the assembly, and by introducing a debonding zone, disc shaped, simulating the non-adherent silver layer.

The highlights of the "silver print test" are its simplicity of implementation (with a simple stencil, a commercial silver paint and a brush), and its possible use when the coating process implies relatively high substrate temperatures (till about 950 °C). For these reasons it is certainly applicable to other situations (in particular for measuring the cohesion of very cohesive coatings), and also to many other coating processes (PVD, CVD, PECVD…). This method could certainly be standardized.

Acknowledgment

We gratefully acknowledge the Région Limousin (France) for Raphaël Bernardie's and Reda Berkouch's Research scholarships.

Nomenclature

σ_r : Strength to rupture
F_b : Force reached at breaking
$A_{C/S}$: Area of the coating/substrate interface
$A_{C/G}$: Area of the coating/glue interface
C_g : Cohesion of the glue

References

[1] T. R. Hull, J. S. Colligon and A. E. Hill, Measurement of thin film adhesion, *Vacuum*, 37 (1987) 327-330.
[2] Z. Chen, K. Zhou, X. Lu and Y. C. Lam, A review on the mechanical methods for evaluating coating adhesion, *Acta Mech.*, 225 (2014) 431-452.
[3] M. JalaliAzizpour, H. MohammadiMajd, M. Jalali and H. Fasihi, Adhesion strength evaluation methods in thermally sprayed coatings, *International Scholarly and Scientific Research & Innovation*, 6 (2012) 337-339.
[4] M. Mellali, P. Fauchais and A. Grimaud, Influence of sub-

strate roughness and temperature on the adhesion/ cohesion of alumina coatings, *Surf. Coat. Technol*., 81 (1995) 275-286.

[5] ASTM C633-13, Standard Test Method for Adhesion or Cohesion Strength of Thermal Spray Coatings, ASTM International, West Conshohocken, PA, *Annual Book of ASTM Standards* (2013) Doi: 10.1520/C0633.

[6] C. C. Berndt, Tensile adhesion testing methodology for thermally sprayed coatings, *J. Mater. Eng*., 12 (1990) 151-158.

[7] J. Cai, Q. Guan, P. Lv, X. Hou, Z. Wang and Z. Han, Adhesion strength of thermal barrier coatings with thermal-sprayed bondcoat treated by compound method of high-current pulsed electron beam and grit blasting, *J. Therm. Spray Technol*., 24 (2015) 798-806.

[8] A. Kishi, S. Kuroda, T. Inoue, T. Fukushima and H. Yumoto, Tensile test specimens with a circumferential precrack for evaluation of interfacial toughness of thermal-sprayed coatings, *J. Therm. Spray Technol*., 17 (2008) 228-233.

[9] J. Lesage and D. Chicot, Role of residual stresses on interface toughness of thermally sprayed coatings, *Thin Solid Films*., 415 (2002) 143-150.

[10] C. K. Lin and C. C. Berndt, Measurement and analysis of adhesion strength for thermally sprayed coatings, *J. Therm. Spray Technol*., 3 (1994) 75-104.

[11] S. Q. Guo, D. R. Mumm, A. M. Karlsson and Y. Kagawa, Measurement of interfacial shear mechanical properties in thermal barrier coating systems by a barb pullout method, *Scr. Mater*., 53 (2005) 1043-1048.

[12] M. Sexsmith and T. Troczynski, Peel adhesion test for thermal spray coatings, *J. Therm. Spray Technol*., 3 (1994) 404-411.

[13] G. Qian, T. Nakamura, C. C. Berndt and S. H. Leigh, Tensile toughness test and high temperature fracture analysis of thermal barrier coatings, *Acta Mater*., 45 (1997) 1767-1774.

[14] M. Watanabe, S. Kuroda, K. Yokoyama, T. Inoue and Y. Gotoh, Modified tensile adhesion test for evaluation of interfacial toughness of HVOF sprayed coatings, *Surf. Coat. Technol*., 202 (2008) 1746-1752.

[15] V. A. Lavrenko, A. I. Malyshevskaya, L. I. Kuznetsova, V. F. Litvinenko and V. N. Pavlikov, Features of high-temperature oxidation in air of silver and alloy Ag − Cu, and adsorption of oxygen on silver, *Powder Metall. and Met. Ceram*., 45 (2006) 476-480.

[16] F. Goutier, S. Valette, A. Vardelle and P. Lefort, Behaviour of alumina-coated 304L steel in a Waste-to-Energy plant, *Surf. Coat. Technol*., 205 (2011) 4425-4432.

[17] S. Valette, A. Denoirjean and P. Lefort, Plasma sprayed steel: Adhesion of an alumina film via a wüstite interlayer, *Surf. Coat. Technol*., 202 (2008) 2603-2611.

[18] R. Bernardie, S. Valette, J. Absi and P. Lefort, Mechanical characterization of alumina coatings on C35 steel, *Surf. Coat. Technol*., 276 (2015) 677-685.